Vazquez et al. Progress in Earth and Planetary Science (2018) 5:75
https://doi.org/10.1186/s40645-018-0229-y

Progress in Earth and Planetary Science

RESEARCH ARTICLE Open Access

Influence of substrate and temperature on the crystallization of KNO_3 droplets studied by infrared thermography

Patricia Vazquez*, Lucas Sartor and Céline Thomachot-Schneider

Abstract

Salt crystallization is a major agent of deterioration in buildings, especially important when belonging to a city's cultural heritage. The study of this process is therefore essential to understand the decay evolution and to establish a correct preservation protocol to avoid future interventions. KNO_3 is a salt found commonly associated to other salts in weathered areas of buildings. In order to recognize the presence of this salt without sampling, the crystallization of KNO_3 was assessed by means of a new non-destructive tool, the infrared thermography. The supersaturation necessary for the nucleation of crystals was obtained by evaporation of solution droplets that allowed the recording of all the processes with an infrared thermography camera. The droplets were tested at different temperatures by placing them on an electric plate at 20 °C and 50 °C to simulate real conditions of building stones placed outdoors and also at 75 °C to emulate extreme situations of stones in arid environments. The droplets evaporated from four different substrates all of them with different interstitial properties: a black 3M tape frequently used as a reference substrate in similar works, a glass slide, and a marble plate with two different artificial finishes, polished and sawed. Thus, the contact angle was around 30° on the glass substrate, over 60° on the 3M tape and the polished marble, and close to 90° in the case of the sawed marble. Results highlighted the usefulness of the infrared thermography in the study of crystallization processes. The exothermic reaction associated to crystallization was too low to be observed, and only punctual heat release spots were recorded. However, a creeping process that creates efflorescence crystallization was clearly observed as an intermittent decrease in the thermographic signal preferentially at high temperatures. The contact angle of the droplet with the surface played an important role in the crystallization type (crystal shape, location, spreading length) when comparing different substrates (i.e., glass and black tape). The different test temperatures revealed different behaviors related to the substrate. The solution spread more at 20 °C on the black tape creating efflorescences while at 50 °C this kind of crystals formed on the stone with both finishes. At 75 °C, the solution spread uniformly over the surface of the glass slide while crystals grew on the top of preexisting ones for the three other substrates with higher contact angle.

Keywords: Infrared thermography, Salt crystallization, Potassium nitrate, Creeping, Efflorescence, Evaporation

* Correspondence: patricia.vazquez@univ-reims.fr
GEGENAA EA 3795, University of Reims Champagne – Ardenne, 2, Esplanade Roland Garros, 51100 Reims, France

Introduction

The understanding of salt behavior is an essential topic in the past and current research due to their contribution in several phenomena affecting everyday life. Thus, the knowledge of salt crystallization and phase change are essential for many fields such as catalysis, energy storage, food research, building stability, and durability and artwork conservation (Telkes 1980; Barta et al. 1986; Graber et al. 1999; Benavente et al. 2004; Aquilano et al. 2016). Several salts such as sodium chloride, sodium sulfate, magnesium sulfate, or gypsum are the center of current researches due to their interest for the society in the mentioned fields. Nevertheless, the intricate processes associated to their formation make necessary the use of complex and high-resolution techniques to achieve further knowledge (Hamilton and Menzies 2010; Saidov et al. 2012; Derluyn et al. 2014; Vázquez et al. 2015). Nitrates are associated to the damage observed in cultural heritage although their studies are less spread (Maguregui et al. 2008). Regarding the current environment and the salt distribution in stone buildings and artworks, nitrate sources are related to pollution (Maguregui et al. 2008; Gibeaux et al. 2018) as industry and diesel shoots affecting mainly areas of high traffic concentration (Lebret et al. 2000). Another nitrate source in buildings is the capillary rising water, especially in an agricultural environment, with fertilizers and animal fecal rests rich in this substance (Curt et al. 2004). Due to the high solubility of nitrates and the fact that KNO_3 crystallizes in high relative humidity (up to 95% at 20 °C and up to 75% at 75 °C), this salt can be found not only in the surface but also within the porous network, independently of the total porosity, the pore size, and distribution in the rocks. Even very compact stones can be affected by the damage caused by nitrate crystallization, as the case of basalt, granite, or marble (Dei et al. 1999).

The thermodynamic conditions vary in relation to the porous media. Crystallization of potassium nitrate in porous stones results in an exothermic reaction, while thermal reaction was not observed in calcareous compacted stones such as marble (Dei et al. 1999). Even within porous stones, the thermal behavior differs from the porous network. The study on cooling solutions also reported temperature variations during crystallization (Barta et al. 1986). Therefore, the study of single droplets becomes necessary in order to understand the crystallization processes without medium constraints and in stable conditions.

The use of infrared thermography (IRT) has been widely adopted over the last several years in many fields such as medicine, chemistry, and security, and it is a basic tool in civil engineering which works even for those requiring special attention as in the case of cultural heritage due to its non-destructive character (Avdelidis and Moropoulou 2004; Bodnar et al. 2013; Bagavathiappan et al. 2013). One of the last applications of this technique was laboratory detection of moisture and salts (Gomez-Heras et al. 2013; Thomachot-Schneider et al. 2016; Lelarge et al. 2017) and the study of salt crystallization from evaporation droplets (Parsa et al. 2015; Vázquez et al. 2014; Vázquez et al. 2015; Vazquez et al. 2018; Sartor et al. 2017) and also in buildings of cultural heritage (Lerma et al. 2014).

Vázquez et al. (2015) presented the study by IRT of sodium chloride from an evaporating droplet, with the differentiation of three phases in relation to the thermosignal variation. Some chemical processes trigger heat exchange reactions such as water evaporation (endothermic reaction) or crystallization (exothermic reaction). Nevertheless, this energy is not always strong enough to be detected by the IRT camera. The crystallization from a droplet entails a variation in shape and consequently in emissivity which allows observing other phenomena of the crystallization process (Vázquez et al. 2014; Vázquez et al. 2015; Vazquez et al. 2018). The variation in shape during evaporation is strongly related to the interface droplet substrate and may condition the evaporation and crystallization process (Shahidzadeh-Bonn et al. 2008).

The aim of this research is to deepen the understanding of the crystallization process of KNO_3, which conducts material deterioration of cultural heritages preferentially in urban areas. For this purpose, the evaporation of single droplets was assessed by IRT at different temperatures and on different substrates.

Methods/experimental

The experimental setup is shown in Fig. 1. In this study, the crystallization of KNO_3 droplets was analyzed by means of a FLIR SC655 long-wave infrared thermography camera operating in the wavelengths 7.5–14 μm and with a detection temperature ranging from − 40 to 150 °C with a sensitivity of 0.1 °C. The detector is an uncooled array of microbolometers. The image size is 640 × 480 pixels, and the noise signal is approximately 40 mK. As in previous works (Vázquez et al. 2015), the recorded signal is called thermosignal (TS). The TS depends on the temperature and emissivity and is expressed in isothermal units (IU). All measurements were undertaken using the passive IRT mode, i.e., without external changing stimulus. All the processes experimented by the droplets were recorded at constant temperature. Prior tests concluded that the optimal recording speed (frame rate) was one image per second throughout the test for the conditions used. The images were treated and analyzed with the ResearchIR software (FLIR).

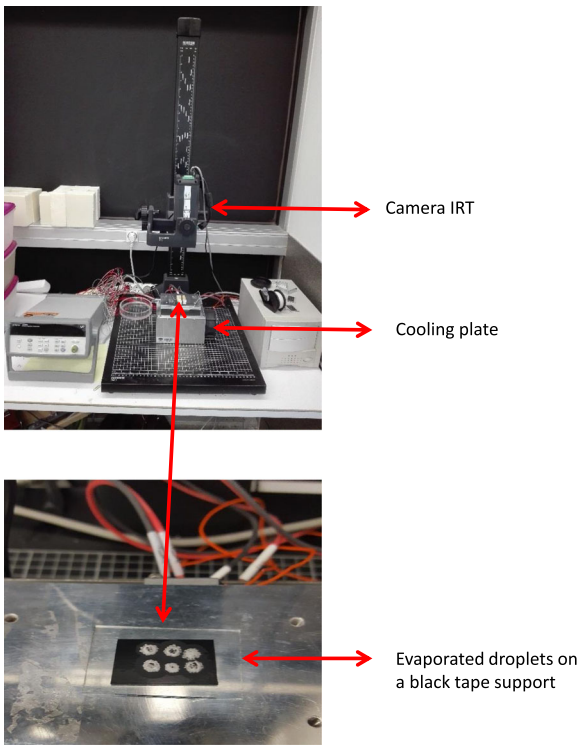

Fig. 1 Experimental setup

The supersaturation needed for the crystallization was obtained by the evaporation of the solvent. Six droplets were dropped in a determinate substrate with a micropipette (5 μL) in each test. KNO_3 solutions were prepared with distilled water at saturations of 80% at three different temperatures of 20 °C, 50 °C, and 75 °C (purity of > 99%, Sigma Aldrich). These solutions were prepared at the same temperature than the substrates, and the 80% saturation was chosen to avoid the possible nucleation by cooling during the process of placing the droplet on the support.

Twelve different tests were conducted combining three temperatures of 20 °C, 50 °C, and 75 °C and four substrates: industrial black tape (3M), microscopy glass slide, polished Amarillo Triana marble, and sawed Amarillo Triana marble. The black adhesive tape was stuck on a microscopy glass slide, and the droplets were dropped on it. This material served as a reference (Vázquez et al. 2015) since its emissivity was determined to be 0.96 in the wavelength analyzed by the camera. On the other three substrates, a small piece of this 3M tape was also stuck to serve as reference point. The glass slide was the one used to make microscope thin sections. The Amarillo Triana marble is a yellow marble with < 1% porosity (Vázquez et al. 2013). Samples were 2 × 2 × 0.1 mm, with the same thickness than the glass slide for glass and 3M tests and showed two artificial finishes (saw and polish). All the supports were cleaned with alcohol before each test to minimize the presence of impurities.

The use of four different substrates, among them also stone, had the purpose of determining the differences in solution spreading and crystallization processes between reference materials (black tape and glass) and real stone used in buildings (marble). The different surface roughness and the character more or less hydrophilic or hydrophobic of the materials lead to a different contact angle between the droplet and the substrate. This angle seems to condition the crystallization process and the crystal patterns (Shahidzadeh-Bonn et al. 2008). For that reason, the contact angle between the droplets and the four substrates was measured at room conditions (20 °C) on 10 droplets for each substrate.

Test temperatures were set constant with the help of cooling plate Tetech CP-061 with a precision of 0.01 °C. The substrates were placed on the cooling plate until they reached the equilibrium with the environment at the set temperature (20 °C, 50 °C, and 75 °C). The sample temperature was measured with thermocouples with a precision of 0.05 °C. In the experimental setup, the risks associated to environmental variations were minimized (control of temperature, humidity, and light). Nevertheless, some variables were introduced due to the human factor of some tasks such as the deposition of the droplets.

Once the droplets crystallized, the crystal morphology and distribution were assessed by optical microscopy with the aid of an Olympus SZH-ILLB stereomicroscope with a digital Tri-CCD camera (Sony, DXP 930) and image analysis software Saisam from Microvision Instruments.

Results

Contact angle measurements

Average and standard deviation of 10 contact angle measurements are shown in Table 1.

The lowest value corresponded to the glass support, i.e., the most hydrophilic, with a wide difference with the rest of materials. The black tape, used as reference in some related studies (Vázquez et al. 2014, Vázquez et al. 2015), showed higher values but slightly lower than the marble whatever its surface finish. Dei et al. (1999)

Table 1 Average and standard deviation of contact angle of KNO3 droplets in four different supports. $N = 10$

Support	Average	St. Dev.
Black tape	68	3
Glass	33	3
Saw marble	89	9
Polished marble	74	5

measured contact angles of 30° for sandstones and 50° for calcareous stones. That can be interpreted as the black tape having similar values to a slightly porous stone. The sawed sample showed an almost vertical angle with the support while the polished marble with softer and flatter surface presented lower values.

Droplet shape

After crystallization, four different zones were detected. Figure 2 shows the thermal image of the droplet and the visible photograph with the different zones. From the inside to outside, the first one was the inner circle (A), in which the crystals were well-formed due to the longer permanence of the solution. They showed mainly acicular or needle shape. This habitus is typical when salt crystallizes in a non-porous system (Dei et al. 1999) and is known as the stable phase of KNO_3 which in this case were all the supports. The second visible zone corresponded to the liquid droplet edge, and in this area (B), the crystals precipitated as a crown of higher relief that surrounds the crystals. The third area was the efflorescence area (C) that exhibited visible crystals with variable shape formed by the solution spreading out of the droplet edge. The last zone, not always observable, corresponded to the halo (D), in which no crystals were visible through a binocular microscope but show a shadow that indicated crystal formation. The halo spread further than the efflorescences.

The dimensions of these four zones have been measured to compare the droplet behavior related to the different substrates and temperatures (Fig. 3). The number of measurements was variable in relation to the droplet though a minimum of three values was required for each zone in each of the six droplets. The results are shown in Table 2.

The tests at different temperatures revealed variations in crystal shape and spreading. As observed in Figure 3 and corroborated by the results in Table 2, at low temperatures, the crystals in the droplet center (A) were longer. Due to the big size of these crystals and the fact that the rest of the solution tended to flow out of the edge, zone B appeared deformed and its dimension was difficult to observe and measure. The efflorescences spread through the support at low temperatures while they grew preferentially in height at high temperatures except for the glass. Evaporation was faster at 50 °C and 75 °C and produced the crystallization of efflorescences on the top of pre-existent crystals (zone B). The halo was hardly visible at low temperatures as the residual solution precipitated as efflorescences while at high temperatures the evaporation was too fast to produce visible crystals.

Regarding the substrate, the black tape showed the most homogeneous precipitations while in the glass support the solution spread considerably through the surface, which made difficult to recognize the crystallization pattern, even impossible at 75 °C. The two stone finishes showed similar precipitation shapes, slightly more spread in the polished finish. In both cases, the center ring looked deformed with respect to the black tape and the stone color made it difficult in some occasions to observe and measure the halo.

Thermal response

The image of the droplets just after their deposition revealed a lower TS than the support (Fig. 2a). These differences were due to two factors: temperature and emissivity. Since the laboratory room was set at 20 °C, in the test at 20 °C, no temperature variations existed between the substrates, the droplet edge, and the droplet top. Thus, the lower signal emitted by the droplet was due to emissivity variations. These variations could be due to the shape effect, for which emissions with angles higher than 45 °C were not received by the camera, and thus, the total signal was lower than a flat shape solution. During the test at 50 °C and 75 °C, the substrate was hotter than the environment and this introduced a temperature gradient within the droplet in which the top had lower temperature than the bottom and the edges.

During the process of crystallization from a droplet, different phases could be determined as observed by

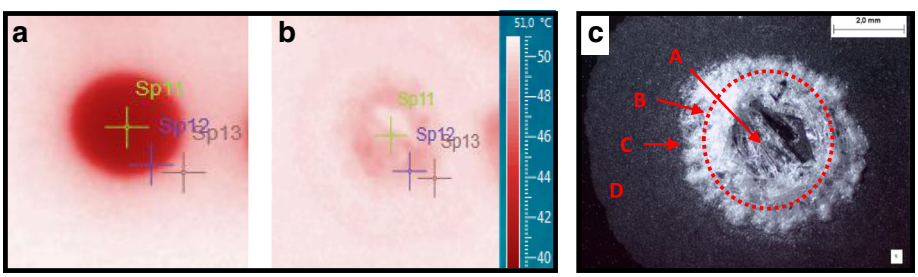

Fig. 2 Droplets observed by IRT and binocular microscope. (**a**) Infrared image of a droplet at the beginning of the test. (**b**) Infrared image of the same droplet after complete evaporation. (**c**) Visual image of the evaporated droplet with the four studied zones

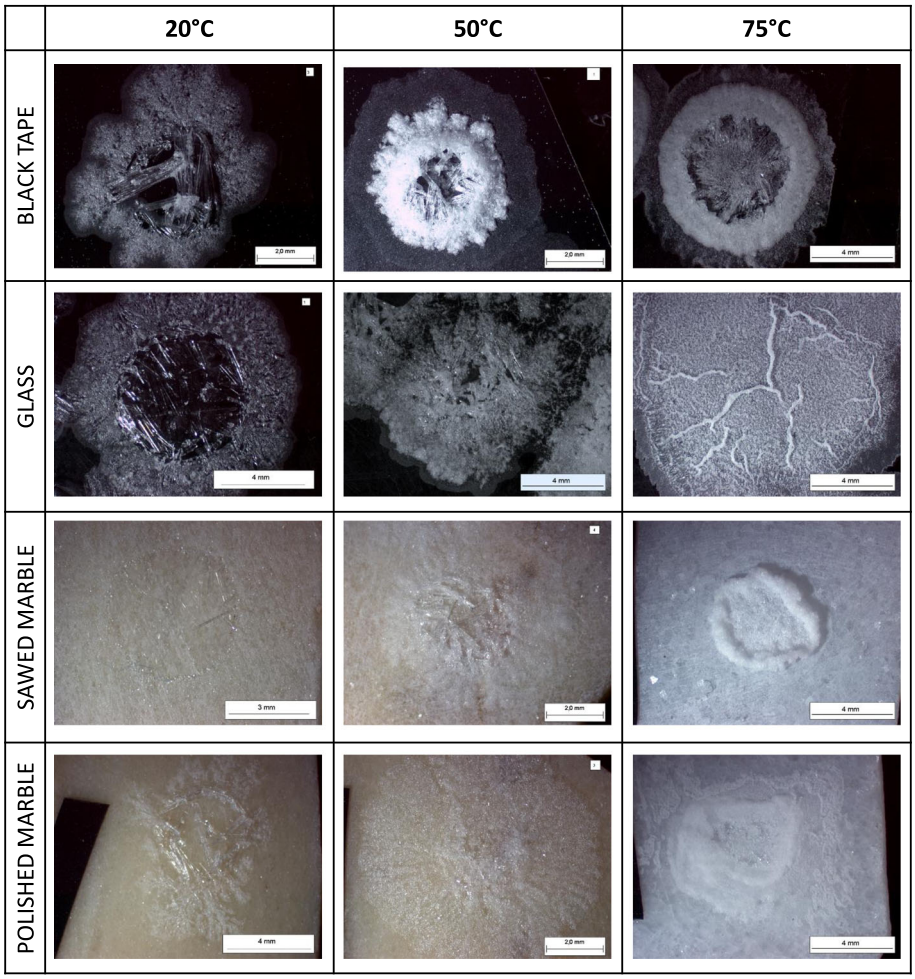

Fig. 3 Evaporated droplets. Pictures of a representative evaporated droplet for each substrate and temperature

IRT. As explained in Vázquez et al. 2015, the thermosignal differences between the droplet and the reference black tape profiles (ΔTS) could be divided into three phases:

Phase I: Homogeneous evaporation of the droplet. The difference of TS between the droplet and the substrate reduced homogeneously and was more evident in the droplet center (Fig. 4a). The droplet became flatter, reducing the emissivity losses, and also thinner, reducing the temperature gradient and approaching the support temperatures. During this phase, some nucleation in the center of the droplet could occur, although the TS emitted was too low to be observed by the IRT.

Phase II: Crystallization. The crystals' shape became visible with or without visible thermal reactions. The TS was still slightly lower than the support due mainly to the relief (Fig. 4) and allows to observe the shape occasionally.

Phase III: Creeping. This phase corresponded to efflorescence growth, and it was easily identified by an

Table 2 Measurements carried out in the four zones of the droplets. Average values from six droplets with at least three measurements for zone and droplet

	Black tape (mm)			Glass (mm)			Sawed marble (mm)			Polished marble (mm)		
Zone	20 °C	50 °C	75 °C	20 °C	50 °C	75 °C	20 °C	50 °C	75 °C	20 °C	50 °C	75 °C
A	2.2	1.2	0.6	3.3	1.0	/	1.6	0.8	/	2.1	1.1	/
B	3.7	3.9	3.6	6.6	2.8*	/	5.8	3.2	2.8	4.8	4.1*	2.6
C	1.6	0.8	1.1	2.2*	1.7	11.4*	/	0.9	0.8	2.4	2.1	0.6
D	0.1*	1.0	0.8	0.2*	0.4*	1.2*	/	/	/	0.5*	/	1.6

A, average of acicular crystals; B, circle diameter; C, average of efflorescence ratio; D, average of halo ratio; * not visible in all the droplets

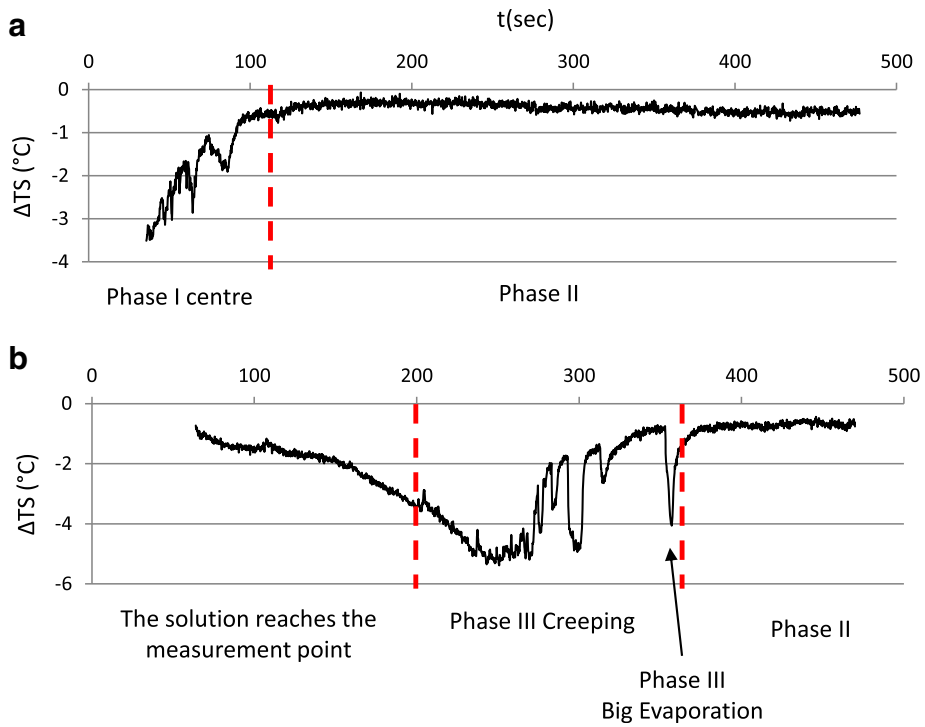

Fig. 4 Representative profiles of a droplet evaporation measured with IRT. **a** IRT profile measured in the droplet center (zone A). **b** IRT profile measured out of the droplet edge (zone C)

intermittent decrease of the TS. Depending on the salt and the temperature, this process may vary in intensity and duration.

Depending on where the TS was recorded, the order of phases may be different from the succession of phase described above for the center of the droplet. For example, in the edge of efflorescence area (zone B), phase I could be missing or creeping (phase III) could occur before crystallization (phase II) (Fig. 4b).

Regarding the zones corresponding to the efflorescence (zone C) and halo area (zone D), at the beginning of the evaporation, the measurement point was placed outside the droplet, on the substrate, and ΔTS was equal or close to zero. When the solution reached the measurement point, the TS became negative since the signal was lower than the black tape. Then, the thermosignal varied. It could show creeping (phase III), an evaporation of the solution $\Delta TS = 0$, a crystallization $\Delta TS < 0$, or even the three processes.

Discussion

The differences in the final shape of the crystallized droplets in relation to the temperature and the support indicated that the formation processes were also different (Gomez-Heras and Fort 2007; Shahidzadeh-Bonn et al. 2008). The thermal response probed these behaviors.

The thermal response was similar for the six droplets of each test. The representative profiles obtained from each temperature, on each support, and for three zones (center, edge, and halo) were drawn in Figs. 5, 6, and 7.

Concerning the profiles measured in the droplet center, the first remark was focused on the starting point. As mentioned above, the top of the droplet had a lower TS than the reference material. This difference was higher with hotter temperature due mainly to the temperature gradient inside the droplet. In all the cases, two stages could be observed in the homogeneous evaporation part (phase I) that corresponded to the slope from the initial point to the stabilization. Within this line, there was a first part in which the ΔTS decreased uniformly (slope ascendant) that corresponded to the homogeneous evaporation of the solution with time. This was followed by the second stage expressed as a sudden decrease (slope ascended almost vertically) followed by a horizontal stabilization, which indicated a final evaporation leading to a crystal ($\Delta TS < 0$) or the substrate ($\Delta TS = 0$). In some of the cases, the ΔTS increased again after a great time interval (slope descendant in Fig. 5, polished). That could be due to the intrusion of a growing crystal in the measuring point in which the solution evaporated and the measurement was done on the support until the intrusion. This phenomenon was not observed at 20 °C due to the long duration of the test in these conditions but it was clearly observed in the 50 °C and 75 °C tests.

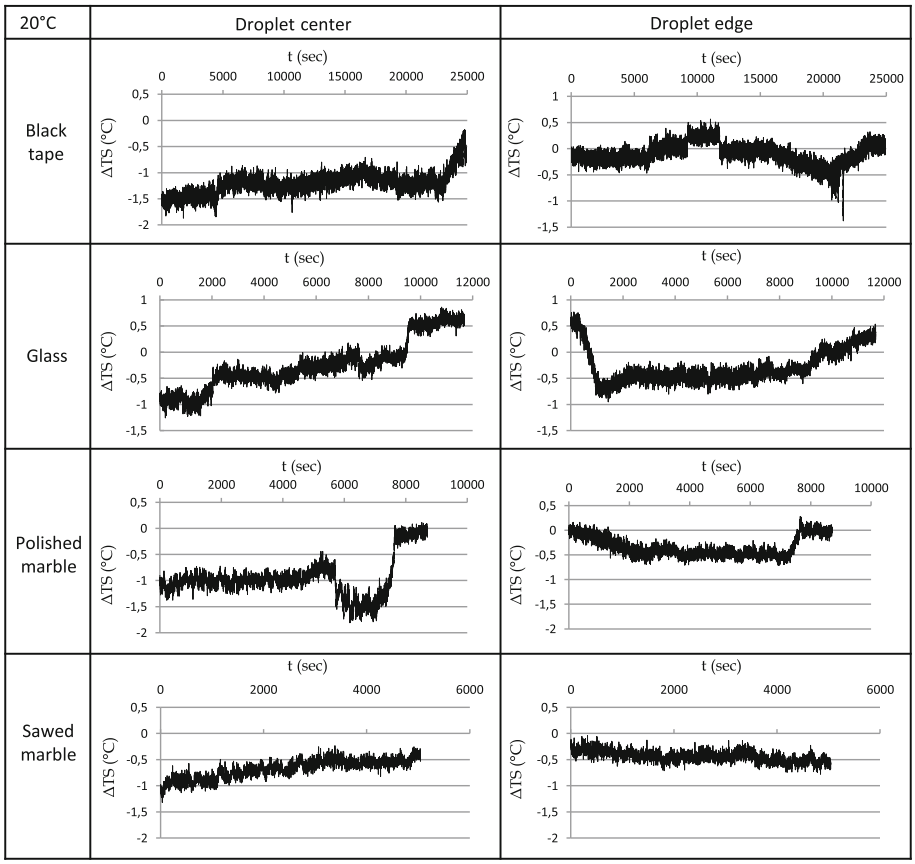

Fig. 5 IRT profiles of each droplet zone at 20 °C for each substrate

The efflorescence and halo areas were sometimes easier to observe on the IRT images than on the visible light ones as in the case of marbles. However, in the IRT image, when the halo was very thin, it could be confounded with the efflorescence area due to energy irradiance of the signal. The thermosignal profiles for the edge and halo measurement points varied in relation to temperature. At 20 °C, the profiles were more or less stable with small irregularities that indicated the arrival of the solution and the crystallization of a layer of crystals that did not interfere too much in the TS. At 50 °C and 75 °C, the signals' amplitude was wider and gave place to interpretation. As in the droplet center, the differences of ΔTS were higher at 75 °C due to the temperature change from the environment to the support. The TS could start in the substrate or in the edge of the droplet since the heat emission close to the edge made it difficult to delimitate the real threshold. If the measurement point was placed on the support (ΔTS = 0), a descent of the profile line was measured due to the arrival of the solution. Then, a fast increase with or without previous creeping was observed until stabilization below ΔTS = 0, which indicated crystal formation.

Regarding temperature, at 20 °C, the TS amplitude was very small and the different phases were less evident. However, phases I and II were recognizable. No creeping was observed at this temperature.

At 50 °C, the droplets tested on the black tape showed clearly all the phases described above, and both stones showed similar behavior despite their different finish and contact angle. The droplets tested on the glass had an erratic behavior explained by the low contact angle and the wide spread of the solution. A flash that corresponded to crystallization energy release was observed punctually at 50 °C; however, due the lack of repeatability in this study, no information was provided.

For all the droplet measured points at 75 °C, the stabilization was not the final stage. The reactions continued in the whole droplet due to the ascension of the solution and the precipitation on the top of preexistent crystals (Vázquez et al. 2015). Due to that, the measuring point can be stable on a crystal during a time interval followed by a new decrease when a new crystal precipitated on it. Thus, in the black tape and the glass, more than one phenomenon of crystallization was measured as confirmed by three steps in the descending

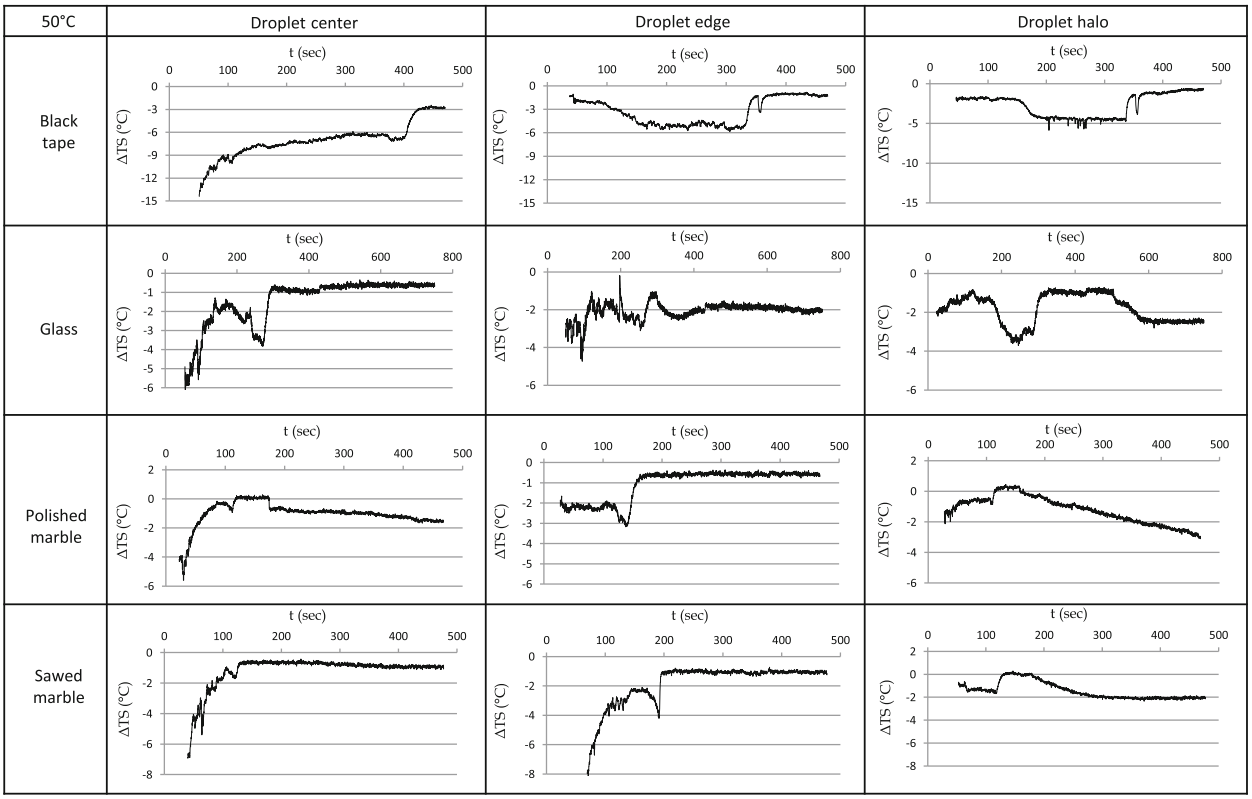

Fig. 6 IRT profiles of each droplet zone at 50 °C for each substrate

slope. The halo TS followed the same pattern than the efflorescence, also with some associated creeping.

Regarding the substrate, the glass and the polished marble had a hydrophilic surface that entailed a higher spreading of the solution. Due to that, creeping was observed even in the droplet center, with crystallization of a very thin film of solution.

The most important observation in the crystallization of KNO_3 was the presence of a large and fast evaporation stage in most of the droplets, independent of the zones and the temperatures. Before stabilization, with or without previous creeping, a final decrease in the slope followed by a rapid increase preceded the crystal formation. This evaporation was not localized punctually but experimented by the whole droplet. This phenomenon was not observed in other salts (Vázquez et al. 2015, Sartor et al. 2017, Vazquez et al. 2018) and requires further research.

Another difference regarding other salts was the visualization of the creeping in the outer efflorescences and the halo. In other salts such as NaCl (Vázquez et al. 2015), the creeping phenomenon was observed only at high temperatures, when efflorescences grow on the top of preexistent crystals on the droplet edge. In KNO_3 droplets, the creeping was clearly observed and strong TS was measured on the spread solution out of the droplet and also in the halo zone, which may indicate that the energy absorption for the evaporation needed to form the crystals is bigger than for other salts.

Conclusions

IRT probed to be an efficient tool to study salt crystallization. The study of KNO_3 evaporation at different temperatures and substrates revealed essential information to understand this salt behavior. Thus, the thermal response of salt crystallization could be studied in situ and, thus, according to the substrate type (porosity, artificial finish, treatments), to determine the type of salt that appeared on the stone.

For KNO_3, the thermosignal and thermal phenomena were more intense with higher temperatures. The different phases of crystallization, i.e., homogeneous evaporation, crystal formation, and creeping, were clearly observed. The latter was measured from the solution that spread out from the droplet edge. In addition, a big evaporation before signal stabilization was observed in the whole droplet for a representative number of samples and for all temperatures and substrates. This evaporation phenomenon can be considered as a special thermal signature of KNO_3 that will allow to recognize this salt crystallization in situ. Efflorescences were found out of the edge for all the droplets but also on the top of preexistent crystals for the high-temperature tests. The

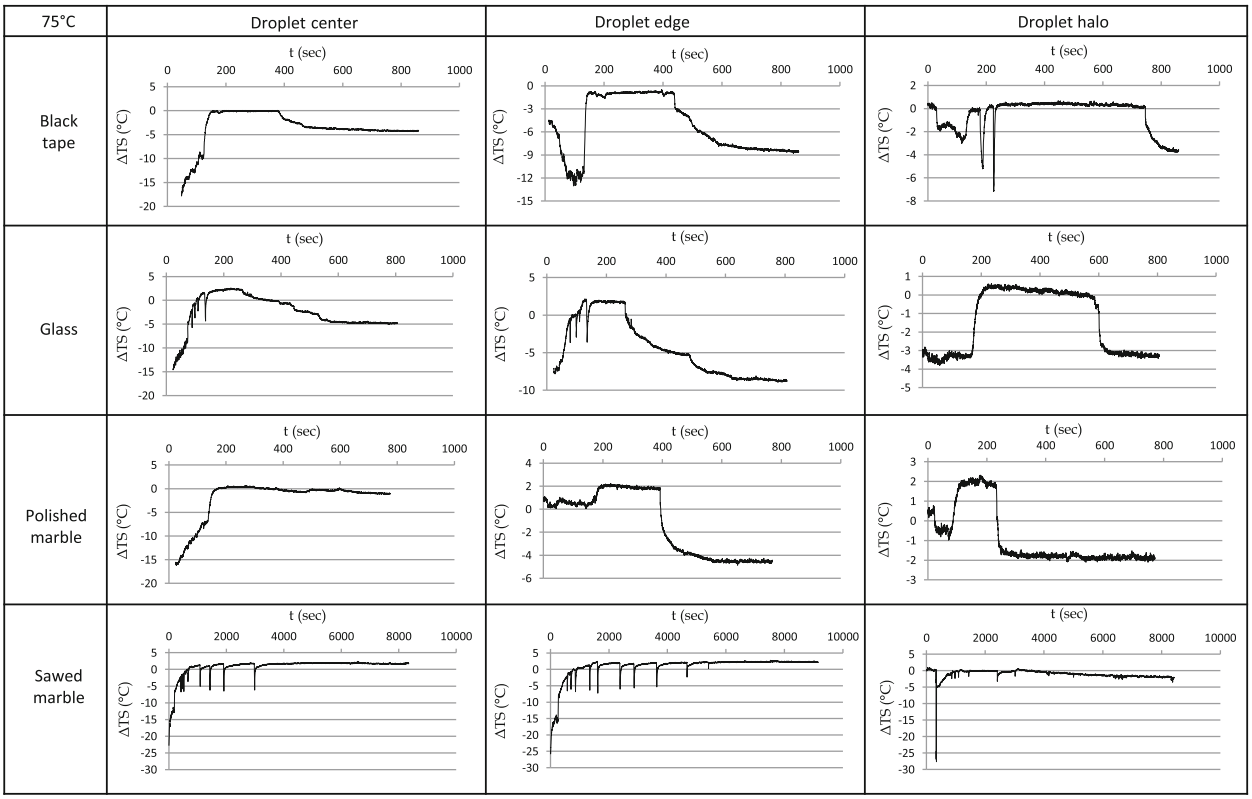

Fig. 7 IRT profiles of each droplet zone at 75 °C for each substrate

heat release due to crystallization was punctually observed though it was not repeatable.

The contact angle of the droplet with the surface played an important role especially if data are compared to contrasted substrates (i.e., glass and black tape). Among narrow contact angles (i.e., black tape and marble), the crystallization was more dependent on the substrate properties than on the angle values.

Temperature revealed different behaviors related to the substrate. The solution spread more at 20 °C in the black tape that led to efflorescence apparition while at 50 °C they were visible on the stone surfaces. At 75 °C, crystals grew on the top of preexistent ones for the three supports with a higher contact angle, while for the glass the solution spread uniformly through the surface.

The study of the KNO_3 thermal response revealed that the crystallization as efflorescence and the crystal spreading through the surface, one of the main problems related to this salt in stone building decay, depends on the specific surface, the stone properties, and the temperature. Low temperature entails a wider spreading of the efflorescences while higher temperature leads to thicker and concentrated ones.

Abbreviations

IRT: Infrared thermography; TS: Thermosignal

Acknowledgements

PV and CS gratefully acknowledge the grant from PEPS to attend the JpGU symposium 2017 held at Tokyo, Japan. LS gratefully acknowledges the travel grant from American Geoscience Union to attend the JpGU symposium 2017 held at Tokyo, Japan.

Funding

This work was supported by the University of Reims Champagne – Ardenne.

Availability of data and materials

Data sharing is not applicable to this article as no datasets were generated or analyzed during the current study.

Authors' contributions

PV proposed the topic and conceived and designed the study. LS carried out the experimental study. PV and LS analyzed the data and helped in their interpretation. CS collaborated with the corresponding author in the construction of the manuscript. All authors read and approved the final manuscript.

Authors' information

PV PhD is an associate Professor at the University of Reims Champagne – Ardenne (France) since 2012. Her research topic is the understanding of the stone deterioration processes at a grain scale, and one of the main decay agents is salt crystallization. In 2013, she got a project to develop IRT in the detection of salt crystallization processes and the consequent stone deterioration. She already published and submitted works about sodium chloride and sodium sulfate.

Competing interests

The authors declare that they have no competing interests.

Publisher's Note

Received: 9 January 2018 Accepted: 10 October 2018
Published online: 15 November 2018

References

Aquilano D, Otálora F, Pastero L, García-Ruiz JM (2016) Three study cases of growth morphology in minerals: halite, calcite and gypsum. Prog Crys Growth Char Mat 62(2):227–251

Avdelidis NP, Moropoulou A (2004) Applications of infrared thermography for the investigation of historic structures. J Cult Her 5(1):119–127

Bagavathiappan S, Lahiri BB, Saravanan T, Philip J, Jayakumar T (2013) Infrared thermography for condition monitoring–a review. Inf Phys Tech 60:35–55

Barta Č, Pokorná Z, Rodová M, Trnka J, Tříska A (1986) Crystallization of KNO_3 under conditions of diffusive and convective regime. Adv Space Res 6(5):1–4

Benavente D, García-del-Cura MA, Fort R, Ordóñez S (2004) Durability estimation of porous building stones from pore structure and strength. Eng Geol 74:113–127

Bodnar JL, Mouhoubi K, Di Pallo L, Detalle V, Vallet JM, Duvaut T (2013) Contribution to the improvement of heritage mural painting non-destructive testing by stimulated infrared thermography. Eur Phys J App Phys 64(1):11002

Curt MD, Aguado P, Sánchez G, Bigeriego M, Fernández J (2004) Nitrogen isotope ratios of synthetic and organic sources of nitrate water contamination in Spain. Water Air Soil Pollut 151(1–4):135–142

Dei L, Mauro M, Baglioni P, Manganelli Del Fà C, Fratini F (1999) Growth of crystal phases in porous media. Langmuir 15(26):8915–8922

Derluyn H, Dewanckele J, Boone MN, Cnudde V, Derome D, Carmeliet J (2014) Crystallization of hydrated and anhydrous salts in porous limestone resolved by synchrotron X-ray microtomography. Nucl Inst Methods Phys Res Sec B 324:102–112

Gibeaux S, Thomachot-Schneider C, Eyssautier-Chuine S, Marin B, Vazquez P (2018) Simulation of acid weathering on natural and artificial building stones according to the current atmospheric SO_2/NO_x rate. Env. Earth Sci 77(9):327

Gomez-Heras M, Fort R (2007) Patterns of halite (NaCl) crystallisation in building stone conditioned by laboratory heating regimes. Environ Geol 52(2):259–267

Gomez-Heras M, Garcia Morales S, Fort R (2013) Integración de datos de termografía de infrarrojos y otras técnicas no destructivas en detección de humedades y sales. Jornada de Técnicas de Reparación y Conservación del Patrimonio 11

Graber TA, Taboada ME, Alvarez MN, Schmidt EH (1999) Determination of mass transfer coefficients for crystal growth of nitrate salts. Crys Res Tech 34(10): 1269–1277

Hamilton A, Menzies RI (2010) Raman spectra of Mirabilite, Na2SO4· 10H2O and the rediscovered metastable Heptahydrate, Na2SO4· 7H2O. J Raman Spectr 41(9):1014–1020

Lebret E, Briggs D, van Reeuwijk H, Fischer P, Smallbone K, Harssema H, Kriz B, Gorynski P, Elliott P (2000) Small area variations in ambient NO_2 concentrations in four European areas. Atm Env 34:177–185

Lelarge N, Thomachot-Schneider C, Mouhoubi K, Bodnar JL, Vazquez P. (2017) Abstract HTT22–03 presented at the JpGU-AGU Joint Meeting 2017, Makuhari, Japan, 20–25 May 2017. https://confit.atlas.jp/guide/event/jpguagu2017/subject/HTT22-03/class?cryptoId=. Accessed 1 Sept 2017

Lerma C, Mas Á, Gil E, Vercher J, Peñalver MJ (2014) Pathology of building materials in historic buildings. Relationship between laboratory testing and infrared thermography. Mater Constr 64(313):009

Maguregui M, Sarmiento A, Martinez-Arkarazo I, Angulo M, Castro K, Arana G, Etxebarria N, Madariaga JM (2008) Analytical diagnosis methodology to evaluate nitrate impact on historical building materials. Anal Bioanal Chem 391(4):1361–1370

Parsa M, Harmand S, Sefiane K, Bigerelle M, Deltombe R (2015) Effect of substrate temperature on pattern formation of nanoparticles from volatile drops. Langmuir 31(11):3354–3367

Saidov TA, Espinosa-Marzal RM, Pel L, George WS (2012) Nucleation of sodium sulfate heptahydrate on mineral substrates studied by nuclear magnetic resonance. J Crys Growth 338(1):166–169

Sartor L, Vazquez P, Schneider-Thomachot C, (2017) Infrared thermography and contact angle as a tool to assess potassium nitrate crystallization; Abstract HTT22–04 presented at the JpGU-AGU Joint Meeting 2017, Makuhari, Japan, 20–25 May 2017. https://confit.atlas.jp/guide/event/jpguagu2017/subject/HTT22-04/class?cryptoId=. Accessed 1 Sept 2017

Shahidzadeh-Bonn N, Rafaı S, Bonn D, Wegdam G (2008) Salt crystallization during evaporation: impact of interfacial properties. Langmuir 24(16):8599–8605

Telkes M (1980) Thermal energy storage in salt hydrates. Solar Energy Materials 2(4):381–393

Thomachot-Schneider C, Gommeaux M, Lelarge N, Conreux A, Mouhoubi K, Bodnar JL, Vázquez P (2016) Relationship between Na2SO4 concentration and thermal response of reconstituted stone in the laboratory and on site. Env Earth Sci 75(9):1–12

Vázquez P, Luque A, Alonso FJ, Grossi CM (2013) Surface changes on crystalline stones due to salt crystallisation. Env earth sci 69(4):1237–1248

Vazquez P, Thomachot-Schneider C, Mouhoubi K, Bodnar J.L, Avdelidis N.P, Charles D, Benavente D (2018) Sodium sulfate crystallisation monitoring using IR thermography. Inf Phy Tech 89(2018):231-241

Vázquez P, Thomachot-Schneider C, Mouhoubi K, Fronteau G, Gommeaux M, Benavente D, Barbin V, Bodnar JL (2015) Infrared thermography monitoring of the NaCl crystallization process. Inf Phy Tech 71:198–207

Vázquez P, Thomachot-Schneider C, Mouhoubi K, Gommeaux M, Fronteau G, Barbin V, Bodnar JL (2014) Study of NaCl crystallization using infrared thermography. In: SWBSS 3rd International Conference on Salt Weathering of Buildings and Stone Sculptures, Brussels